HHS Public Access

Author manuscript

Cancer Res. Author manuscript; available in PMC 2022 April 15.

Published in final edited form as:

Cancer Res. 2018 April 15; 78(8): 2014–2025. doi:10.1158/0008-5472.CAN-17-2063.

ERα-mediated nuclear sequestration of RSK2 is required for ER+ breast cancer tumorigenesis

Katarzyna A. Ludwik[1], **Oliver G. McDonald**[1], **David R. Brenin**[2], **Deborah A. Lannigan**[1,3,‡]

[1]Department of Pathology, Microbiology and Immunology, Vanderbilt University Medical Center, Nashville, TN 37232

[2]Department of Surgery, University of Virginia, Charlottesville, VA 22908

[3]Department of Cell and Developmental Biology, Vanderbilt University, Nashville, TN 37232

Abstract

Although ribosomal protein S6 kinase A3 (RSK2) activation status positively correlates with patient responses to anti-estrogen hormonal therapies, the mechanistic basis for these observations is unknown. Using multiple in vitro and in vivo models of ER+ breast cancer, we report that ERα sequesters active RSK2 into the nucleus to promote neoplastic transformation and facilitate metastatic tumor growth. RSK2 physically interacted with ERα through its N-terminus to activate a pro-neoplastic transcriptional network critical to the ER+ lineage in the mammary gland, thereby providing a gene signature that effectively stratified patient tumors according to ERα status. ER+ tumor growth was strongly dependent on nuclear RSK2, and transgenic mice engineered to stably express nuclear RSK2 in the mammary gland developed high grade ductal carcinoma in situ. Mammary cells isolated from the transgenic model and introduced systemically successfully disseminated and established metastatic lesions. Anti-estrogens disrupted the interaction between RSK2 and ERα, driving RSK2 into the cytoplasm and impairing tumor formation. These findings establish RSK2 as an obligate participant of ERα-mediated transcriptional programs, tumorigenesis, and divergent patient responses to anti-estrogen therapies.

Keywords

RSK2; p90 ribosomal S6 kinase; p90RSK; ERα; cyclin D1; breast cancer; growth factors; anti-estrogens; organoids; transgenic mice

Introduction

Intrinsic or therapy-induced resistance to endocrine-targeted therapy for estrogen receptor positive (ER+) breast cancer is a major obstacle to improving patient outcomes (1). Therefore, there is an ongoing effort to identify predictive biomarkers that will indicate responsiveness to therapy. ERK1/2 in response to growth factor and cytokine signaling

‡Corresponding author : D.A. Lannigan, Ph.D., Vanderbilt University Medical Center, Tel: 615-322-4560, deborah.lannigan@vanderbilt.edu, Address: 771 Preston Research Building, 2220 Pierce Ave, Nashville, TN 37232-6840.

D.A.L. declares a potential conflict of interest. Other authors do not have a conflict of interest.

initiates a phosphorylation cascade that results in the activation of the Ser/Thr protein kinase, p90RSK (RSK) (2, 3). Interestingly, active RSK correlates with disease-free survival and response to chemotherapy in ER+ breast cancer (4, 5). The kinase domains of the four members that comprise the RSK family are very similar but family members appear to have both redundant and separate contributions to development, homeostasis and disease etiologies (6, 7). RSK controls several oncogenic processes, including proliferation, viability and motility and, therefore, has accordingly been implicated in the etiology of numerous cancers including breast (8–16). However, despite detailed knowledge on RSK oncogenic functions, the mechanistic rationale that underpins the correlation of active RSK with endocrine-based responsiveness in ER+ breast cancer remains an enigma.

Here we report that ERα physically interacts with RSK2, resulting in accumulation of RSK2 in the nucleus. This interaction activates a transcriptional network that is critical for ER+ tumor growth and provides a gene signature that stratifies patient tumors according to ER+ status. Anti-estrogens disrupt the association of ERα and RSK2 and drive RSK2 into the cytoplasm, which results in severely impaired tumorigenic capacity. Furthermore, forced nuclear RSK2 in a novel transgenic mouse model triggers neoplastic transformation of ER+ epithelial cells within the native mammary gland. Taken together, our results reveal that the nuclear sequestration of RSK2 by ERα activates a pro-neoplastic transcription program that is susceptible to disruption by anti-estrogen therapy. These data provide a mechanistic explanation for the clinical observations that RSK2 correlates with responsiveness to endocrine-based therapies.

Materials and Methods

Additional experimental procedures, antibodies, and reagents are listed in Supplementary Data.

Animals

All procedures involving animals were done in accordance with current federal (NIH Guide for Care and Use of Laboratory Animals) and university guidelines and were approved by the University of Virginia and Vanderbilt University Institutional Animal Care and Use Committee.

C57BL/6J mice carrying a transgene composed of the mouse mammary tumor virus-long terminal repeat (MMTV-LTR) linked to sequences encoding the hemagglutin (HA) tag, the NLS from SV40 (PKKKRKV) and murine RSK2 (MMTV-HA-NLS-RSK2) were generated by the University of Virginia Gene Targeting and Transgenic Facility (C57BL/6J$^{\text{MMTV-HA-NLS-RSK2}}$). Ten backcrosses were performed to wild type C57BL/6J. At 12 wk, 6m, or 16m virgin female MMTV-NLS-RSK2 or wild type mice were euthanized and the mammary glands analyzed.

Cell culture and treatment

Mycoplasma free MCF-7, BT-474 and ZR-75-1 cells were obtained, cultured and authenticated as directed by American Type Culture Collection (ATCC). Cells were serum starved and treated as described in Supplementary Data.

Single epithelial cells were isolated from the mammary glands of sixteen month old mice and spheres cultured as described (17). For 2 passages (every 9 days) spheres were dissociated with 1x trypsin and equal number of cells from WT and NLS-RSK2 spheres were re-plated. Alternatively, p0 spheres (day 9) were transduced with GFP-luciferase and after three days the linearity of the bioluminescence signal was tested (15).

Clinical Samples

The Cooperative Human Tissue Network (CHTN) provided the human breast cancer tissue and clinical data. Every CHTN institution has obtained human subjects assurance from the Office of Human Research Protections, DHHS. The Assurance document provides agreement that the institution will comply with federal human subjects regulations (The "Common Rule;" 45 CFR part 46). Each Division of the CHTN is approved by its local Institutional Review Board (IRB) to collect and distribute biospecimens. The IRBs review the procedures in place to ensure adequate protection of human subjects and protection of patient privacy and confidentiality. The approvals are reviewed by the IRB yearly. Samples are described in (Table S1) and assessment for ERα and progesterone receptor (PR) and HER2 amplification is described in the Supplementary Data. In some cases organoids were prepared from the tissue (18).

Immunostaining and immunodetection

Indirect and direct fluorescence samples were stained as described (15, 18) and an overview is provided in the Supplementary Data.

Immunoprecipitation

MCF-7 cells treated with the dimethyl-3,3′-dithiobispropionimidate (5mM in PBS (30 min)) were quenched in 50mM Tris pH8.0, 150mM NaCl (10min). The insoluble fraction was obtained (19). Lysates were incubated with 2μg rabbit anti-ERα, rabbit IgG (1h, 4°C) followed by MagnaBind goat anti-rabbit IgG magnetic beads (50μl, 1h, 4°C) or anti-GFP mAb-magnetic beads (50μl, 1h, 4°C). Alternatively, lysates were incubated with GFP-Trap®_M (ChromoTek GmbH) (18μl, 1h, 4°C) pre-bound with GFP-GST protein (150ng, 1h, 4°C). The immunoprecipitate was washed 2x with buffer (50mM Tris pH8.0, 150mM NaCl, 5mM EDTA, 1% Triton X-100, 0.1% deoxycholate) and 3x with the same buffer without detergents. The beads were boiled (19). GST-fusion proteins were purified using glutathione sepharose 4B (300μl;) and stored (−20°C) in storage buffer (20mM HEPES pH 7.4, 300mM NaCl, 1mM EGTA, 1mM DTT, 50% glycerol).

RNASeq

Total RNA extraction (RNeasy Kit) was performed on serum starved cells treated with EGF ((10nM)/E_2(1nM) for 8h) and quality controlled using Agilent 2100 Bioanalyzer (RIN 8). Libraries were constructed (TruSeq RNA Library Prep Kit), and sequenced (Illumina HiSeq 2500 at the Vanderbilt VANTAGE Core). Raw reads were aligned to the human reference genome hg38 (Genome Reference Consortium GRCh38) and differential gene expression analyzed using CLC Workbench 10.0. Genes with absolute fold change>2.5 and

false discovery rate (FDR) <0.05 were considered to be significantly DE. RNA-Seq data is available at Gene Expression Omnibus under accession: GSE99707.

Gene expression data from patients with invasive breast carcinoma (TCGA version 1/11/2015) were analyzed using Morpheus. Samples were filtered to include primary tumors from patients with infiltrating ductal carcinoma. Z-scores were calculated for each ER+ patient by adding z-scores of genes down regulated in RSK2-KO cells and subtracting z-scores of genes up-regulated in RSK2-KO cells. RSK2-low tumors have RSK2 z-score <0, and RSK2-high tumors RSK2 z-score>0. Hierarchical clustering of patient samples using one minus the Spearman's rank correlation and total linkage was performed using the RSK2_529 set. iRegulon1.3 (Cytoscape 3.5.0) was used for transcription factor prediction. STRING10.5 (confidence 0.7) was used to predict and identify functional nodes of protein networks. GSEA was performed with javaGSEA software (Broad Institute) using expression of all detected genes (16,394) in RSK2-KO versus WT cells against gene signatures from the Molecular Signature Database v6.0 (20).

Statistical Analysis

Statistical analyses were performed using GraphPad Prism 6.0a.

Results

Nuclear active RSK2 in invasive ER+ breast cancer

We first addressed activation and localization of RSK by immunofluorescence (IF) across a panel of 25 invasive ER+ breast cancer patient samples. Active nuclear RSK was observed in ~ 70% of these samples (Fig. 1A, S1A and Table S1) and, within these samples, the intensity of nuclear RSK was strongly correlated with the intensity of ERα (Fig. 1B). Cyclin D1 levels and ERα were also correlated (Fig. 1A, B, S1A), consistent with observations that cyclin D1 is frequently over-expressed in ER+ cancers (21). Because IF provides a quantitative readout, we conclude that there is a positive linear relationship between the levels of active nuclear RSK and ERα in ER+ breast cancer.

Antibodies against active RSK cannot distinguish between different RSK isoforms, since the phosphorylation sites responsible for activation are identical (6). An anti-RSK2 antibody identified that RSK2 was localized to the nucleus in those ER+ tumor samples containing active nuclear RSK (Fig. 1C). A specific anti-RSK1 antibody suitable for IF was not available and therefore, we used human ER+ cell lines to examine RSK1 and RSK2 nuclear translocation. In response to growth factors and cytokines, endogenous activated RSK2 accumulated in the nucleus (Fig. 1D, S1B–S1D), as did C-terminally fluorescently tagged RSK2 (Fig. S1E). In contrast, nuclear accumulation was not observed for RSK1 (Fig. S1E) despite both isoforms being active (Fig. S1F) and reports of RSK1 nuclear translocation (22). Taken together, we conclude that RSK2 is the active isoform present in the nucleus in invasive ER+ breast cancer tumor samples.

RSK2-regulated gene signature correlates with invasive ER+ breast cancer

RNAi knockdown experiments revealed that RSK2 was essential for ER+ tumor growth and expression of cyclin D1 in an MCF-7 orthotopic model (Fig. 1E, F, S1G). To identify the mechanistic basis of these findings, we employed CRISPR/Cas9 gRNA targeting to genetically delete RSK2 in MCF-7 cells (RSK2-KO; Fig. S2A). RSK2-KO MCF-7 cells showed reduced proliferation relative to wild type (WT) controls, which could be rescued by ectopic expression of RSK2 (Fig. S2B). Addition of the ERα degrader, fulvestrant, reduced proliferation to the same extent in WT and RSK2-KO MCF-7 cells (Fig. 2A). These results indicated that ERα-dependent proliferation is partly controlled by RSK2, since knockout of RSK2 did not result in a further reduction of proliferation at high concentrations of fulvestrant. Next, we performed RNA sequencing (RNA-seq) on RSK2-KO and WT MCF-7 cells that were treated with a cocktail containing estradiol (E_2) and EGF, in order to explore transcriptomic changes under conditions where both ERα and RSK2 are active. This analysis identified 529 differentially expressed (DE) genes in the RSK2-KO cells relative to WT (RSK2_529; Table S2, Fig. S2C). We confirmed the specificity of the DE by quantitative RT-PCR of selected genes, which was further validated with rescue by overexpression of RSK2 in the RSK2-KO cells (Fig. S2D). Gene set enrichment analysis (GSEA) demonstrated that genes up regulated in invasive ductal breast cancer versus ductal carcinoma in situ (DCIS) were significantly enriched in WT versus RSK-KO (FDR q-value < 0.05) (Fig. 2B) (23–25). To test whether the directionality of changes of the RSK2_529 set were reflected in ER+ breast cancer patients, we calculated z-scores in ER+ patients with high and low RSK2 mRNA expression. Patient Z-scores were higher in RSK2-high compared to RSK2-low patients demonstrating that in ER+ breast cancer patients expression of the RSK2_529 set is correlated with RSK2 mRNA levels and that the direction of the effect of expression is concordant with that of the RSK2_529 set (Fig. 2C). Unsupervised hierarchical clustering of the RSK2_529 set across 782 breast cancer gene expression sets in the TCGA dataset revealed that patients were stratified into two major clusters, based on their positivity for ERα (Fig. 2D). Hypergeometric enrichment probability analyses further showed that the RSK2_529 set separated the ER+ patients with a probability of $5.8*10^{-69}$ and the ER− patients with a probability of $1.0*10^{-75}$ (two tailed Fisher's exact test $p< 0.0001$; Table S3) (26). These hypergeometric probabilities are in a similar range to those obtained with PAM50, a 50-gene intrinsic subtype classifier (27), and the luminal versus basal signature (28) (Table S3). There is <1% overlap between the RSK2_529 set and PAM50 ($p>0.05$ two-tailed Fisher's exact test) indicating that the RSK2_529 set is distinct from PAM50. The RSK2_529 set shares ~ 10% of the genes with those found in the luminal versus basal signatures, which indicates the importance of RSK2 to the luminal lineage (Fig. S2E). In contrast to results obtained with the RSK2_529 set, the signatures obtained from tissue homeostasis (29, 30), ductal versus lobular invasive carcinoma (31), or estrogen receptor related 1− gene set (32) failed to distinguish between ER+ and ER− patients (Table S3). Proliferation and cell cycle genes (29, 30) did not significantly contribute to the RSK2_529 set as shown by GSEA (FDR q-value>0.05) (Fig. S2F) and their removal did not substantially reduce the high enrichment probabilities for separating ER+ from ER− patients (Fig. S2G and Table S3).

The RSK2 signature was further reduced to 212 DE genes (RSK2_212) by taking into account transcript level abundance. Analysis of the RSK2_212 set by iRegulon (33) and the STRING 10.0 database identified a network of genes consisting of 127 DE genes (RSK2_127) that were regulated by GATA3, FOXA1, EP300 and ESR1 (ERα gene). These results are in agreement with GSEA analysis, which identified that E_2-responsive genes are enriched in WT versus RSK2-KO (FDR q-value < 0.05) (Fig. 2E) (34). GATA3, FOX1 and EP300 are regulators of ERα function (35–41) and high mRNA and protein expression of GATA3 and FOXA1 are associated with ER+ breast cancer (42). The RSK2_127 set separated patients based on their ERα status with a greater probability that the RSK2_529 set (Fig. 2F and Table S3). Removal of the 23 genes related to cell cycle and proliferation that were present in the RSK2_127 set improved the hypergeometric probability of distinguishing between ER+ and ER− breast cancer samples (Fig. S2H, S2I). We conclude that RSK2 contributes to ER+ breast cancer through regulation of a subset of the ERα transcriptome.

ERK1/2 and ERα cooperatively control RSK2 nuclear sequestration

RSK2 activates ERα-mediated transcription through physical association and by phosphorylating ERα at Ser-167 (pSer-167) (43). To distinguish whether physical association or pSer-167 was responsible for our transcriptomic findings, we treated MCF-7 cells with the anti-estrogen, 4-hydroxytamoxifen (4-OHT). 4-OHT disrupted the association of RSK2 and ERα without altering pSer-167 (Fig. S3A, S3B), strongly suggesting that the interaction of RSK2 with ERα (rather than pSer-167) is critical to the regulation of the ERα transcriptome. This conclusion was further supported in vivo, as inducible overexpression of ERα with doxycycline in the mammary gland, resulted in increased levels of active nuclear RSK, as predicted based on previous observations that proteins in a complex frequently regulate each other's protein levels (Fig. S3C). Based on these observations we tested whether association of ERα with RSK2 regulated RSK2 nuclear accumulation. Indeed 4-OHT inhibited RSK2 nuclear accumulation by ~ 50–80% across multiple different ER+ breast cancer cell lines, which were sensitive to 4-OHT (Fig. 1D, S1D, S3D–F). Fulvestrant also reduced RSK2 nuclear accumulation (Fig. S3D). In addition to preventing RSK2 nuclear accumulation anti-estrogen treatment was able to drive RSK2 into the cytoplasm after it had accumulated (Fig. S3G). Changes in RSK2 localization did not appear to arise secondary to altered expression levels or activity of RSK2 or ERK1/2 (Fig. S3H). Consistent with the anti-estrogen treatments, silencing ERα also reduced RSK2 nuclear accumulation in response to growth factors (Fig. 3A). Silencing RSK2 did not affect ERα nuclear localization (Fig. S3I), indicating that ERα nuclear accumulation occurs independently of RSK2. To more rigorously test whether ERα controls RSK2 nuclear accumulation we developed a 3D organoid culture system and generated organoids from primary human ER+ breast cancer tissue. Importantly, the levels of ERα, cyclin D1 and activated nuclear RSK were similar to those observed in the patient tissues from which they were derived. Similar to 2D cultures, 4-OHT treatments in 3D resulted in loss of nuclear RSK2 coupled to cytoplasmic accumulation of RSK2 and reduced cyclin D1 levels (Fig. 3B, 3C, S3J, S3K). We conclude that endocrine-based therapies result in dissociation of a complex consisting of RSK2 and ERα and that loss of this interaction reduces RSK2 nuclear accumulation.

Although our data clearly demonstrated that ERα is required for RSK2 nuclear accumulation, E_2 stimulation alone was insufficient (Fig. S3L) and required additional growth factor and cytokine signaling (Fig. 1D, S1B–D). A panel of 80 kinase inhibitors was therefore screened to identify signaling inputs that contribute to RSK2 nuclear localization. Of these, only compounds that inhibited ERK1/2 decreased the levels of nuclear RSK2, which is consistent with the known role of RSK2 in ERK1/2 signaling (Fig. S3M, Table S4). We conclude that ERK1/2 activation allows RSK2 to translocate into the nucleus while ERα interacts and sequesters RSK2 in the nucleus.

The extreme N-terminus of RSK2 is required for interaction with ERα

Because physical association with ERα was required for RSK2 nuclear accumulation, we next wished to identify the region of RSK2 responsible for nuclear accumulation and ERα binding. To this end we took advantage of the observations that the RSK1 isoform does not accumulate in the nucleus, and created chimeras of RSK1 and RSK2, which were fluorescently tagged at their C-terminus (Fig. S4A). A chimera in which the RSK2 C-terminal kinase domain (CTKD) was swapped with that of RSK1 (RSK2(1-407)RSK1(404-735)) retained its ability to accumulate, while a chimera with the reverse swap (RSK1(1-401)RSK2(406-740)) did not accumulate (Fig. 4A, S4B), despite the fact that both chimeras were active (Fig. S4C). Thus the RSK2 residues from 1 to 407 were necessary for RSK2 accumulation. Within this region, the RSK2 residues at the extreme N-terminus (1-67) and in the linker (329-424) diverge the most from those of RSK1 (54% and 68% identity, respectively, compared to 80% overall identity). We therefore hypothesized that either the linker domain or the N-terminus were most likely responsible for nuclear translocation. Replacing the RSK2 linker with that of RSK1 ((RSK2(1-375) RSK1(370-401)RSK2(406-740)) did not alter activity or nuclear accumulation (Fig. 4A, S4B, S4D), suggesting that the linker region did not play a role. Because a deletion mutant of residues from 1 to 67 of RSK2 was highly unstable, we replaced the extreme N-terminal region of RSK1 with that of RSK2 ((RSK2(1-67)RSK1(62-735)). This chimera was both active (Fig. S4C) and accumulated in the nucleus (Fig. 4A, B). In contrast, replacing the extreme N-terminal region of RSK2 with that of RSK1 to create RSK1(1-61)RSK2(68-740) resulted in a chimera that was active (Fig. S4C) yet lost its ability to accumulate in the nucleus (Fig. 4C). We conclude that residues from 1 to 67 are required for RSK2 nuclear accumulation. The RSK2 residues from 1 to 67 on their own could not facilitate accumulation of a heterologous protein in comparison to the nuclear localization signal (NLS) of SV40 (PKKKRKV) (Fig. S4E). Thus the extreme N-terminus is necessary but not sufficient for RSK2 accumulation.

We hypothesized that the RSK2 residues from 1 to 67 are important for RSK2 nuclear accumulation because they are responsible for interaction with ERα. Consistent with this, both RSK2 and the chimera, RSK2(1-67)RSK1(62-735), but not RSK1, co-immunoprecipitated with ERα (Fig. 4D). Additionally, silencing ERα reduced nuclear accumulation of the chimera, similar to the WT (Fig. 4E). The RSK2 region from 1 to 67 is highly conserved within the class Mammalia, as is the analogous region in RSK1 (Fig. S4F). There are two notable differences in the extreme N-terminus between RSK1 and RSK2, which include a Ser-Pro-Ser motif and a five amino acid insert that are present only

in RSK2. A Ser-Pro-Ser motif regulates ERK2 nuclear translocation (44) but mutation of residues within this motif did not alter RSK2 nuclear accumulation (Fig. S4G, H). However, deletion of the five amino acid insert (RSK2Δ27-32) prevented nuclear accumulation (Fig. 4F), without affecting RSK2 activation (Fig. S4I). Moreover, ERα specifically co-associated with a purified, recombinant protein containing the RSK2 residues from 1 to 67 (Fig. 4G). We conclude that the extreme N-terminus interacts with ERα to sequester RSK2 in the nucleus.

Nuclear accumulation of RSK2 promotes ER+ breast cancer growth

Silencing endogenous RSK2 with co-expression of a shRNA-resistant mutant that does not accumulate in the nucleus (rRSK1(1-61)RSK2(68-740)) failed to increase cyclin D1 levels compared to a mutant that localizes to the nucleus (rRSK2(1-67)RSK1(62-735)) (Fig. 5A, S5A). To further verify that RSK2 nuclear accumulation is required to support ER+ breast cancer growth we employed the RSK2 chimeras that did or did not accumulate in the nucleus, which reflects their ability to interact with ERα. As expected, silencing RSK2 in MCF-7 cells strongly impaired tumor growth, and this inhibition was rescued with ectopic expression of WT shRNA-resistant RSK2 (Fig. 5B, S5B). Importantly, restoration of tumor growth was also observed by ectopic expression of the nuclear accumulating chimera but not with the non-accumulating chimera (Fig. 5B, S5B). Nuclear accumulation of the various ectopically expressed fusion proteins (Fig. 5C) was consistent with our *in vitro* data (Fig. 4B, 4C) and their levels were similar (Fig. S5C). As expected, cyclin D1 levels mirrored the ability of the constructs to accumulate in the nucleus, while levels of pSer-167 ERα did not (Fig. 5D). These data are consistent with a RSK2-dependent activation of a gene program that facilitates ER+ breast cancer by physical association rather than ERα phosphorylation at Ser- 167. Collectively, these observations clearly demonstrate that RSK2 nuclear accumulation is required for tumor growth in ER+ breast cancer.

Nuclear accumulation of RSK2 triggers neoplastic transformation

Because nuclear RSK2 was required for ER+ tumor growth, we next asked whether forced expression of RSK2 in the nucleus of non-transformed ER+ mammary epithelia could facilitate neoplastic transformation *in vivo*. To this end a novel transgenic mouse with mammary gland-restricted, nuclear RSK2 expression (MMTV-NLS-RSK2) was generated. The transgene was expressed specifically in the mammary gland and localized to the nucleus (Fig. S6A, S6B). Because mouse models of ER+ breast cancer have a long latency (45), we examined mammary glands at early (six months) and later (sixteen months) time points. At six months, ductal hyperplasia was observed (Fig. S6C, S6D) with expansion of the ER+ mammary population (Fig. S6E). By sixteen months, ducts and lobules were markedly expanded in NLS-RSK2 mice compared to controls (Fig. 6A). Microscopic examination of expanded ducts revealed clear evidence of neoplastic transformation, which was manifested as DCIS. DCIS can be histologically evaluated into a three tiered grading system that is largely based on increasing severity in nuclear morphology. NLS-RSK2 mice showed clearly evidence of high grade DCIS, including solid growth within ducts that obliterated the lumen (Fig. 6B), prominent apoptosis and mitosis including atypical mitotic forms (Fig. 6C, 6D), severe nuclear atypia including nuclear enlargement (6E, 6F), pleomorphism, loss of polarity and stratification (6E). Consistent with these observations IF experiments

detected elevated levels of the S-phase marker, PCNA (Fig. 6G), and the DNA damage marker, γH2AX (Fig. 6H). Approximately 50% of the mice developed high grade ER+ DCIS (Fig. 6I, S6G). To functionally confirm neoplastic transformation we isolated the mammary cells from the sixteen month old NLS-RSK2 and assayed their *in vitro* and *in vivo* tumorigenic capacity. Sphere cultures generated from the NLS-RSK2 mice were more efficient at forming spheres over multiple passages than those obtained from WT mice (Fig. 6J). For the *in vivo* assays spheres generated from WT and NLS-RSK2 mammary glands from passage 0 were transduced with luciferase (Fig. S6H). Intra-cardiac (IC) injection of equal numbers of the transduced spheres into NCG mice resulted in 100% of the mice injected with NLS-RSK2 spheres developing metastatic tumors; whereas, WT spheres failed to form tumors (Fig. 6K, S6I). We conclude that forced nuclear expression of RSK2 triggers in situ transformation of ER+ mammary epithelial cells, and that these cells are capable of tumorigenic growth if removed from the mammary gland.

Discussion

Our studies provide a mechanistic basis for the clinical observations that active RSK correlates, with endocrine-therapy responsiveness and increased overall survival in patients with ER+ breast cancer. ERα interacts with residues from 27 to 32 located in the N-terminus of RSK2 to sequester RSK2 in the nucleus. This motif is highly conserved from Mammalia to Aves, which is a hallmark of residues that are important as functional domains. The interaction of RSK2 with ERα, which is disrupted by mutagenesis of RSK2, anti-estrogens, or silencing ERα, allows ERK1/2-activated RSK2 to accumulate to high levels in the nucleus. Loss of RSK2 from the nucleus results in reduced ER+ tumor formation, which is due to the inactivation of the pro-neoplastic transcriptional network comprised of ESR1, EP300, GATA3 and FOXA1 that is critical to maintain ER+ breast cancer (42, 46). This conclusion is further supported by the ability of the RSK2 gene signature to stratify breast cancer patients according to their ERα status.

RSK2 influences ERα-mediated transcriptional activity via phosphorylation or physical association (43, 47). The residue, Ser-167, within ERα is a RSK phosphorylation site (43) but a correlation between the phosphorylation of Ser-167 and tumor formation was not observed. However, tumor formation was absolutely dependent on RSK2 nuclear accumulation. Similar to the observations with active RSK, the phosphorylation of Ser-167 is correlated with responsiveness to endocrine-based therapies and overall survival (4, 48, 49) but we propose that this phosphorylation is an indirect biomarker for active RSK2 and therefore, is correlated but not causally related to ER+ breast cancer.

Remarkably, forced expression of RSK2 in normal mammary glands triggered the development of high grade DCIS. In this model transformation occurs with a long latency, which is similar to both human breast cancer and many other transgenic mouse models (45, 50). We note that although mice developed high grade DCIS, no invasive tumors were identified, perhaps due to a need for additional time or because further genetic or epigenetic events beyond RSK2 are needed for initial invasion of neoplastic cells through the basement membrane into the surrounding stroma. Interestingly, bypassing the intravasation step, demonstrated that nuclear RSK2 supported metastatic tumor growth, indicating that

RSK2-dependence is likely selected as an early *in situ* event that helps promote neoplastic transformation and remains essential thereafter to support tumorigenesis once invasive tumor growth has been established.

Supplementary Material

Refer to Web version on PubMed Central for supplementary material.

Acknowledgments

We thank Pricilla Furth, M.D. (Georgetown) for providing the CERM mice. We also thank the University of Virginia Research Histology Core and the Biorepository and Tissue Procurement Facility. Tissue samples were provided by the CHTN, which is funded by the National Cancer Institute. Other investigators may have received specimens from the same subjects. Data generated by the TCGA Research Network: http://cancergenome.nih.gov/ was used. This work was supported by NIH grant GM084386 (D.A. Lannigan) and Susan G. Komen Breast Cancer Foundation #IIR12223770 (D.A. Lannigan).

References

1. Clarke R, Tyson JJ, Dixon JM. Endocrine resistance in breast cancer--An overview and update. Mol Cell Endocrinol. 2015; 418 (Pt 3) 220–34. [PubMed: 26455641]
2. Dalby KN, Morrice N, Caudwell FB, Avruch J, Cohen P. Identification of regulatory phosphorylation sites in mitogen-activated protein kinase (MAPK)-activated protein kinase-1a/p90rsk that are inducible by MAPK. J Biol Chem. 1998; 273: 1496–505. [PubMed: 9430688]
3. Jensen CJ, Buch MB, Krag TO, Hemmings BA, Gammeltoft S, Frodin M. 90-kDa ribosomal S6 kinase is phosphorylated and activated by 3-phosphoinositide-dependent protein kinase-1. J Biol Chem. 1999; 274: 27168–76. [PubMed: 10480933]
4. Jiang J, Sarwar N, Peston D, Kulinskaya E, Shousha S, Coombes RC, et al. Phosphorylation of estrogen receptor-alpha at Ser167 is indicative of longer disease-free and overall survival in breast cancer patients. Clin Cancer Res. 2007; 13: 5769–76. [PubMed: 17908967]
5. Moon HG, Yi JK, Kim HS, Lee HY, Lee KM, Yi M, et al. Phosphorylation of p90RSK is associated with increased response to neoadjuvant chemotherapy in ER-positive breast cancer. BMC Cancer. 2012; 12: 585. [PubMed: 23216670]
6. Romeo Y, Zhang X, Roux PP. Regulation and function of the RSK family of protein kinases. Biochem J. 2012; 441: 553–69. [PubMed: 22187936]
7. Ludwik KA, Lannigan DA. Ribosomal S6 kinase (RSK) modulators: a patent review. Expert Opin Ther Pat. 2016; 26: 1061–78. [PubMed: 27410995]
8. Lara R, Mauri FA, Taylor H, Derua R, Shia A, Gray C, et al. An siRNA screen identifies RSK1 as a key modulator of lung cancer metastasis. Oncogene. 2011; 30: 3513–21. [PubMed: 21423205]
9. Smith JA, Poteet-Smith CE, Xu Y, Errington TM, Hecht SM, Lannigan DA. Identification of the first specific inhibitor of p90 ribosomal S6 kinase (RSK) reveals an unexpected role for RSK in cancer cell proliferation. Cancer Res. 2005; 65: 1027–34. [PubMed: 15705904]
10. Clark DE, Errington TM, Smith JA, Frierson HF Jr, Weber MJ, Lannigan DA. The serine/threonine protein kinase, p90 ribosomal S6 kinase, is an important regulator of prostate cancer cell proliferation. Cancer Res. 2005; 65: 3108–16. [PubMed: 15833840]
11. Kang S, Elf S, Lythgoe K, Hitosugi T, Taunton J, Zhou W, et al. p90 ribosomal S6 kinase 2 promotes invasion and metastasis of human head and neck squamous cell carcinoma cells. J Clin Invest. 2010; 120: 1165–77. [PubMed: 20234090]
12. David JP, Mehic D, Bakiri L, Schilling AF, Mandic V, Priemel M, et al. Essential role of RSK2 in c-Fos-dependent osteosarcoma development. J Clin Invest. 2005; 115: 664–72. [PubMed: 15719069]
13. Doehn U, Hauge C, Frank SR, Jensen CJ, Duda K, Nielsen JV, et al. RSK is a principal effector of the RAS-ERK pathway for eliciting a coordinate promotile/invasive gene program and phenotype in epithelial cells. Mol Cell. 2009; 35: 511–22. [PubMed: 19716794]

14. Smolen GA, Zhang J, Zubrowski MJ, Edelman EJ, Luo B, Yu M, et al. A genome-wide RNAi screen identifies multiple RSK-dependent regulators of cell migration. Genes Dev. 2010; 24: 2654–65. [PubMed: 21062900]
15. Ludwik KA, Campbell JP, Li M, Li Y, Sandusky ZM, Pasic L, et al. Development of a RSK Inhibitor as a Novel Therapy for Triple-Negative Breast Cancer. Mol Cancer Ther. 2016; 15: 2598–608. [PubMed: 27528706]
16. Zhou Y, Yamada N, Tanaka T, Hori T, Yokoyama S, Hayakawa Y, et al. Crucial roles of RSK in cell motility by catalysing serine phosphorylation of EphA2. Nat Commun. 2015; 6: 7679. [PubMed: 26158630]
17. Archibald A, Mihai C, Macara IG, McCaffrey L. Oncogenic suppression of apoptosis uncovers a Rac1/JNK proliferation pathway activated by loss of Par3. Oncogene. 2015; 34: 3199–206. [PubMed: 25109337]
18. Pasic L, Eisinger-Mathason TS, Velayudhan BT, Moskaluk CA, Brenin DR, Macara IG, et al. Sustained activation of the HER1-ERK1/2-RSK signaling pathway controls myoepithelial cell fate in human mammary tissue. GEnes & Dev. 2011; 25: 1641–53. [PubMed: 21828273]
19. Groehler AL, Lannigan DA. A chromatin-bound kinase, ERK8, protects genomic integrity by inhibiting HDM2-mediated degradation of the DNA clamp PCNA. J Cell Biol. 2010; 190: 575–86. [PubMed: 20733054]
20. Liberzon A, Birger C, Thorvaldsdottir H, Ghandi M, Mesirov JP, Tamayo P. The Molecular Signatures Database (MSigDB) hallmark gene set collection. Cell Syst. 2015; 1: 417–25. [PubMed: 26771021]
21. Finn RS, Aleshin A, Slamon DJ. Targeting the cyclin-dependent kinases (CDK) 4/6 in estrogen receptor-positive breast cancers. Breast Cancer Res. 2016; 18: 17. [PubMed: 26857361]
22. Gao X, Chaturvedi D, Patel TB. Localization and retention of p90 ribosomal S6 kinase 1 in the nucleus: implications for its function. Mol Biol Cell. 2012; 23: 503–15. [PubMed: 22130794]
23. Subramanian A, Tamayo P, Mootha VK, Mukherjee S, Ebert BL, Gillette MA, et al. Gene set enrichment analysis: a knowledge-based approach for interpreting genome-wide expression profiles. Proc Natl Acad Sci U S A. 2005; 102: 15545–50. [PubMed: 16199517]
24. Mootha VK, Lindgren CM, Eriksson KF, Subramanian A, Sihag S, Lehar J, et al. PGC-1alpha-responsive genes involved in oxidative phosphorylation are coordinately downregulated in human diabetes. Nature genetics. 2003; 34: 267–73. [PubMed: 12808457]
25. Schuetz CS, Bonin M, Clare SE, Nieselt K, Sotlar K, Walter M, et al. Progression-specific genes identified by expression profiling of matched ductal carcinomas in situ and invasive breast tumors, combining laser capture microdissection and oligonucleotide microarray analysis. Cancer Res. 2006; 66: 5278–86. [PubMed: 16707453]
26. Kaddi CD, Parry RM, Wang MD. Multivariate hypergeometric similarity measure. IEEE/ACM Trans Comput Biol Bioinform. 2013; 10: 1505–16. [PubMed: 24407308]
27. Parker JS, Mullins M, Cheang MC, Leung S, Voduc D, Vickery T, et al. Supervised risk predictor of breast cancer based on intrinsic subtypes. J Clin Oncol. 2009; 27: 1160–7. [PubMed: 19204204]
28. Charafe-Jauffret E, Ginestier C, Monville F, Finetti P, Adelaide J, Cervera N, et al. Gene expression profiling of breast cell lines identifies potential new basal markers. Oncogene. 2006; 25: 2273–84. [PubMed: 16288205]
29. Ashburner M, Ball CA, Blake JA, Botstein D, Butler H, Cherry JM, et al. Gene ontology: tool for the unification of biology. The Gene Ontology Consortium. Nature genetics. 2000; 25: 25–9. [PubMed: 10802651]
30. The Gene Ontology C. Expansion of the Gene Ontology knowledgebase and resources. Nucleic Acids Res. 2017; 45: D331–D8. [PubMed: 27899567]
31. Turashvili G, Bouchal J, Baumforth K, Wei W, Dziechciarkova M, Ehrmann J, et al. Novel markers for differentiation of lobular and ductal invasive breast carcinomas by laser microdissection and microarray analysis. BMC Cancer. 2007; 7: 55. [PubMed: 17389037]
32. Stein RA, Chang CY, Kazmin DA, Way J, Schroeder T, Wergin M, et al. Estrogen-related receptor alpha is critical for the growth of estrogen receptor-negative breast cancer. Cancer Res. 2008; 68: 8805–12. [PubMed: 18974123]

33. Janky R, Verfaillie A, Imrichova H, Van de Sande B, Standaert L, Christiaens V, et al. iRegulon: from a gene list to a gene regulatory network using large motif and track collections. PLoS Comput Biol. 2014; 10: e1003731. [PubMed: 25058159]
34. Dutertre M, Gratadou L, Dardenne E, Germann S, Samaan S, Lidereau R, et al. Estrogen regulation and physiopathologic significance of alternative promoters in breast cancer. Cancer Res. 2010; 70: 3760–70. [PubMed: 20406972]
35. Bernardo GM, Lozada KL, Miedler JD, Harburg G, Hewitt SC, Mosley JD, et al. FOXA1 is an essential determinant of ERalpha expression and mammary ductal morphogenesis. Development. 2010; 137: 2045–54. [PubMed: 20501593]
36. Asselin-Labat ML, Sutherland KD, Barker H, Thomas R, Shackleton M, Forrest NC, et al. Gata-3 is an essential regulator of mammary-gland morphogenesis and luminal-cell differentiation. Nat Cell Biol. 2007; 9: 201–9. [PubMed: 17187062]
37. Kouros-Mehr H, Slorach EM, Sternlicht MD, Werb Z. GATA-3 maintains the differentiation of the luminal cell fate in the mammary gland. Cell. 2006; 127: 1041–55. [PubMed: 17129787]
38. Feng Y, Manka D, Wagner KU, Khan SA. Estrogen receptor-alpha expression in the mammary epithelium is required for ductal and alveolar morphogenesis in mice. Proc Natl Acad Sci U S A. 2007; 104: 14718–23. [PubMed: 17785410]
39. Yi P, Wang Z, Feng Q, Pintilie GD, Foulds CE, Lanz RB, et al. Structure of a biologically active estrogen receptor-coactivator complex on DNA. Mol Cell. 2015; 57: 1047–58. [PubMed: 25728767]
40. Metivier R, Penot G, Hubner MR, Reid G, Brand H, Kos M, et al. Estrogen receptor-alpha directs ordered, cyclical, and combinatorial recruitment of cofactors on a natural target promoter. Cell. 2003; 115: 751–63. [PubMed: 14675539]
41. Shang Y, Hu X, DiRenzo J, Lazar MA, Brown M. Cofactor dynamics and sufficiency in estrogen receptor-regulated transcription. Cell. 2000; 103: 843–52. [PubMed: 11136970]
42. Cancer Genome Atlas N. Comprehensive molecular portraits of human breast tumours. Nature. 2012; 490: 61–70. [PubMed: 23000897]
43. Clark DE, Poteet-Smith CE, Smith JA, Lannigan DA. Rsk2 allosterically activates estrogen receptor alpha by docking to the hormone-binding domain. EMBO J. 2001; 20: 3484–94. [PubMed: 11432835]
44. Chuderland D, Konson A, Seger R. Identification and characterization of a general nuclear translocation signal in signaling proteins. Mol Cell. 2008; 31: 850–61. [PubMed: 18760948]
45. Dabydeen SA, Furth PA. Genetically engineered ERalpha-positive breast cancer mouse models. Endocr Relat Cancer. 2014; 21: R195–208. [PubMed: 24481326]
46. Murakami S, Nagari A, Kraus WL. Dynamic assembly and activation of estrogen receptor alpha enhancers through coregulator switching. Genes Dev. 2017; 31: 1535–48. [PubMed: 28887413]
47. Eisinger-Mathason TS, Andrade J, Groehler AL, Clark DE, Muratore-Schroeder TL, Pasic L, et al. Codependent functions of RSK2 and the apoptosis-promoting factor TIA-1 in stress granule assembly and cell survival. Mol Cell. 2008; 31: 722–36. [PubMed: 18775331]
48. Motomura K, Ishitobi M, Komoike Y, Koyama H, Nagase H, Inaji H, et al. Expression of estrogen receptor beta and phosphorylation of estrogen receptor alpha serine 167 correlate with progression-free survival in patients with metastatic breast cancer treated with aromatase inhibitors. Oncology. 2010; 79: 55–61. [PubMed: 21071990]
49. Yamashita H, Nishio M, Kobayashi S, Ando Y, Sugiura H, Zhang Z, et al. Phosphorylation of estrogen receptor alpha serine 167 is predictive of response to endocrine therapy and increases postrelapse survival in metastatic breast cancer. Breast Cancer Res. 2005; 7: R753–64. [PubMed: 16168121]
50. St-Hilaire S, Mandal R, Commendador A, Mannel S, Derryberry D. Estrogen receptor positive breast cancers and their association with environmental factors. Int J Health Geogr. 2011; 10: 32. [PubMed: 21569288]

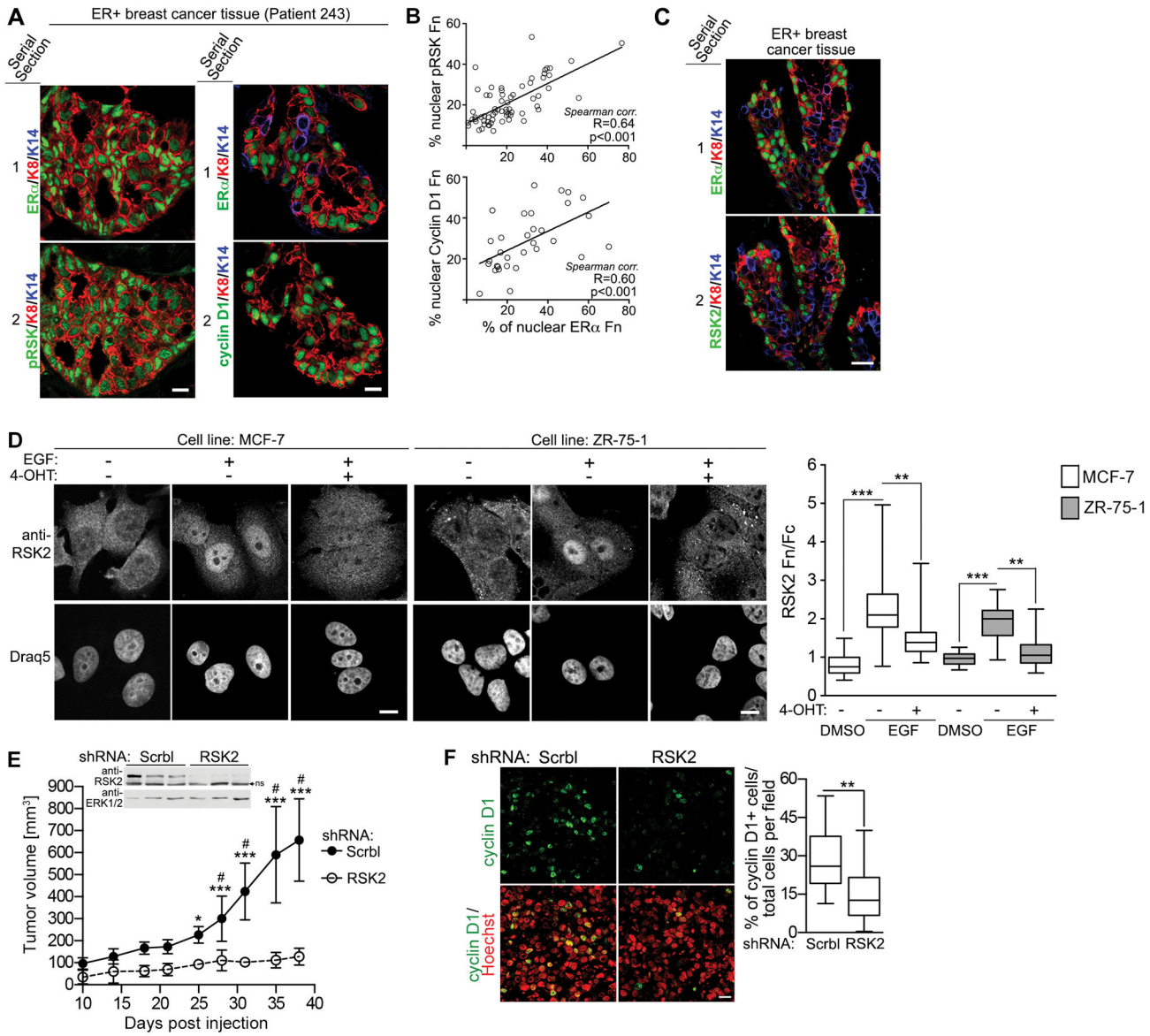

Figure 1. RSK2 in ER+ breast cancer

(A) Serial sections of ER+ breast cancer tissue. Scale bar=20μm. (B) Correlation of ERα nuclear fluorescence intensity (Fn) with nuclear active (pRSK) and cyclin D1. (n=14 patients, ≥3 sections/patient). (C) RSK2 is nuclear in ER+ breast cancer tissue. (D) Anti-estrogens decrease EGF-induced RSK2 nuclear accumulation as measured by Fn to cytoplasmic fluorescence (Fc). MCF-7 and ZR-75-1 were treated with 2 or 10μM 4-OHT, respectively. DNA stained with Draq5. Scale bar=10μm. (Bar, median±quartile, n=3, ≥90 cells/treatment). **p<0.01, ***p<0.001; Student's t-test. (E) RSK2 silencing reduces ER+ tumor growth. Transduced MCF-7 cells were injected into the 4th mammary fat pad of NSG mice implanted with an E_2 pellet. (Symbol, mean±SD, n≥5 mice/group) *p<0.05, ***p<0.001 Scramble (Scrbl) versus RSK2 shRNA; #<0.001 Scrbl (day 0) versus Scrbl (at each time point); two-way ANOVA. (Inset) Analysis of RSK2 levels after tumor isolation. Samples were normalized to ERK1/2. ns=non-specific. (F) Loss of RSK2 decreases the

percentage of cyclin D1+ cells in xenografts. Scale bar=20μm. (Bar, median±quartile, n=4 tumors; ≥5 fields/tumor). **p<0.01 Student's t-test.

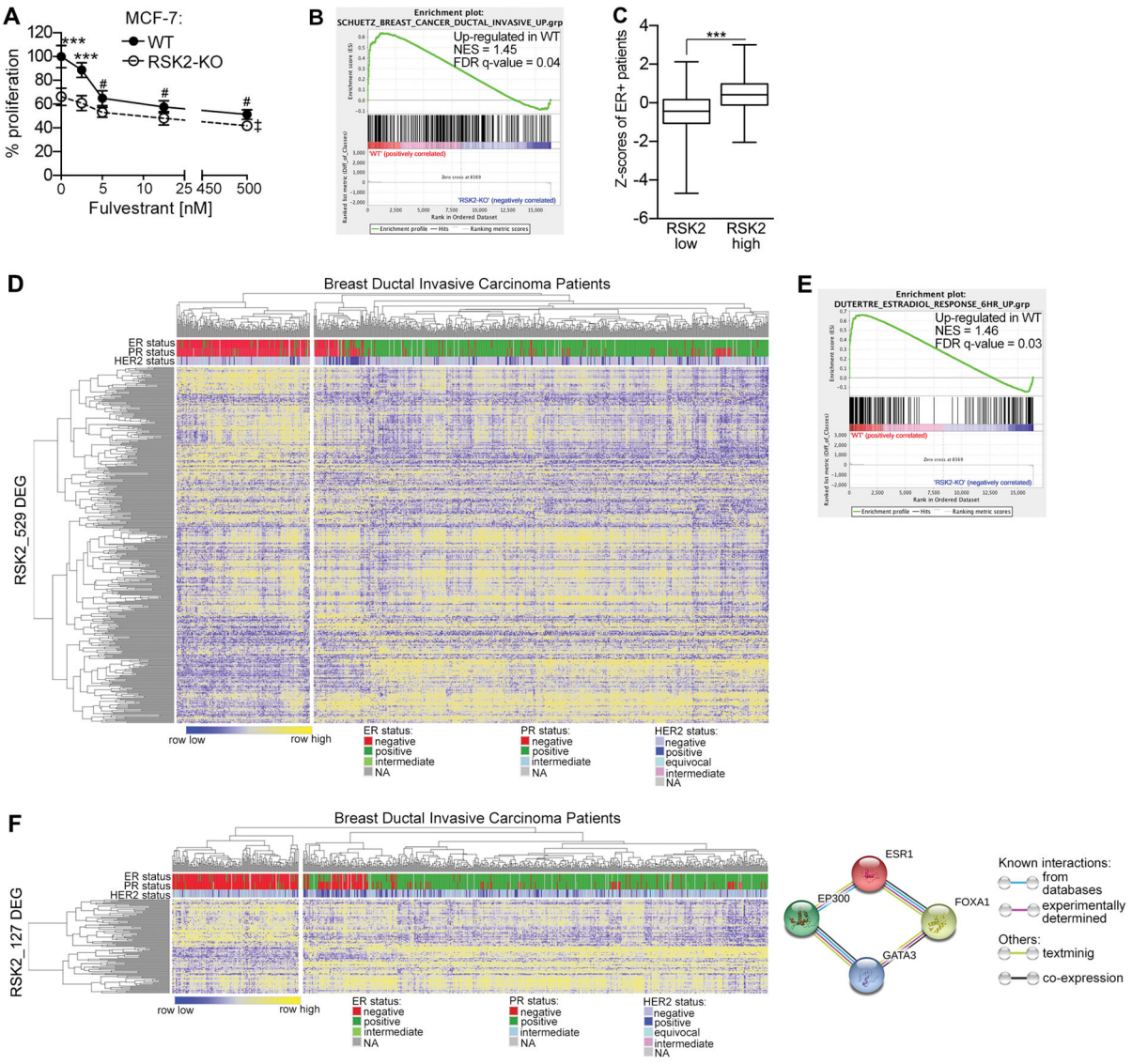

Figure 2. RSK2 gene signature stratifies patients based on ERα status

(A) RSK2 and ERα regulate MCF-7 proliferation via the same pathway. RSK2 was genetically deleted (RSK2-KO) in MCF-7 cells and proliferation measured ± fulvestrant. (Bar, mean±SD, n=3, sextuplicate) ***p<0.001 WT versus RSK2-KO at each concentration; #p<0.001 WT (vehicle) versus WT (fulvestrant), ‡p<0.001 RSK2-KO (vehicle) versus RSK2-KO (Fulvestrant); two-way ANOVA. (B) GSEA plot showing a positive correlation between genes up regulated in invasive ductal carcinoma versus DCIS and genes up regulated in WT versus RSK2-KO cells. (C) Cumulative patient Z-scores were generated for each ER+ patient (TCGA) by adding individual z-scores of genes down regulated in RSK2-KO cells and subtracting individual z-scores of genes up regulated in RSK2-KO cells. Patients were divided into RSK2-low (RSK2 expression z-score<0) (n=254) and RSK2-high (RSK2 expression z-score>0) (n=287) and cumulative patient z-scores plotted. (Bar, median±quartile) ***p<0.001; Student's t-test. (D) Hierarchical clustering of TCGA gene expression data from 782 invasive breast tumors reveals that the RSK2_529 gene

signature stratifies patients according to ERα. Horizontal axis: individual patients; vertical axis: individual genes. White bar separates columns at the first dendrogram split. (E) GSEA plot showing a positive correlation between genes up regulated by estradiol treatment and genes up regulated in WT versus RSK2-KO cells. (F) Hierarchical clustering of TCGA gene expression data from 782 invasive breast tumors reveals that the RSK2_127 gene signature stratifies patients according to the presence of ERα. Horizontal axis: individual patients; vertical axis: individual genes. White bar separates columns at the first dendrogram split. (Inset) The RSK2 regulatory network that is essential to the ER+ lineage.

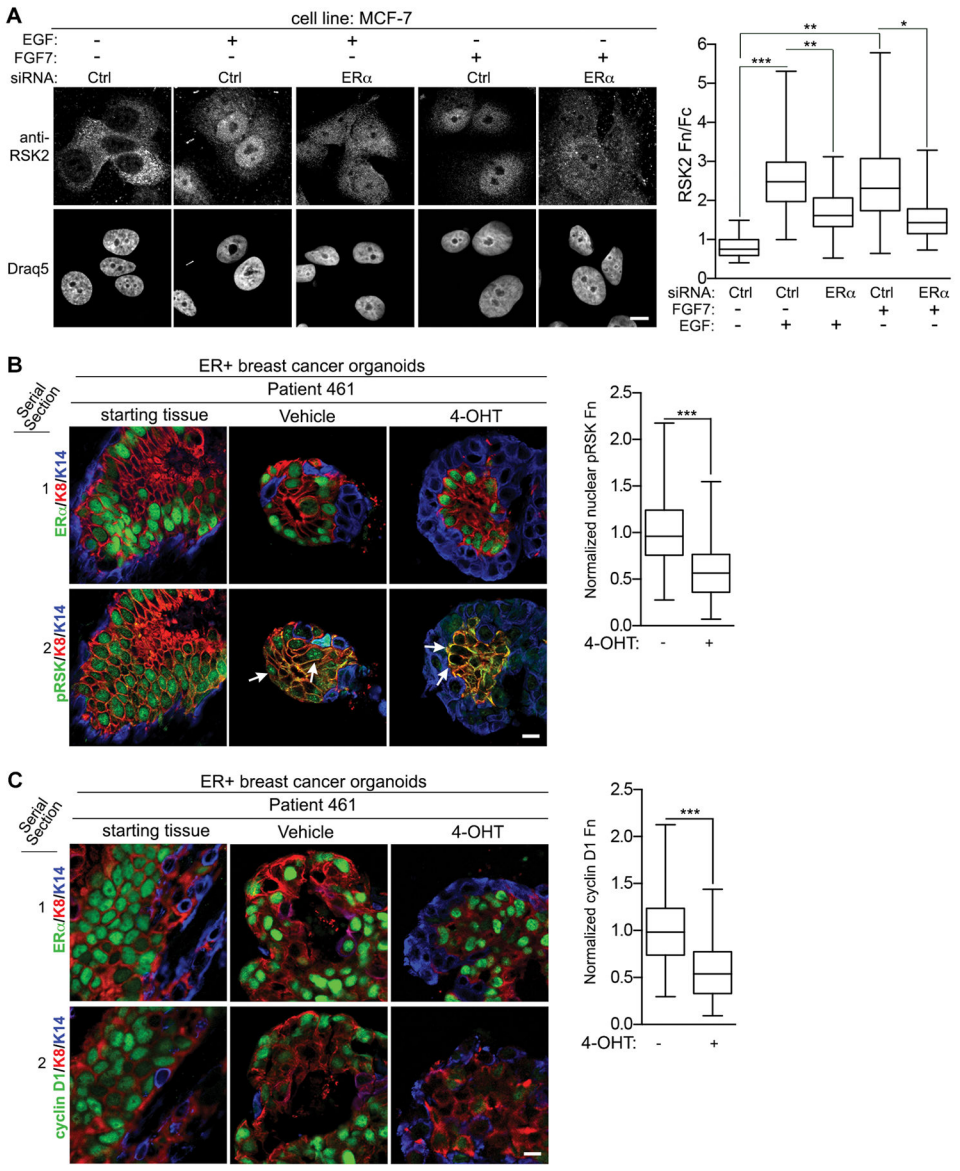

Figure 3. ERα regulates RSK2 nuclear localization

(A) Silencing ERα reduces RSK2 nuclear accumulation. MCF-7 cells transfected with control (Ctrl) or ERα-specific siRNA and treated ± growth factors. Scale bar=10μm. (Bar, median±quartile (n≥3, ≥100 cells/treatment). *p<0.05, **p<0.01, ***p<0.001; Student's t-test. Anti-estrogens decrease nuclear active RSK (B) and cyclin D1 (C) levels in ER+ breast cancer organoids. Serial sections of starting tissues and ER+ breast cancer organoids treated ± 4-OHT. Scale bar=20 μm. Arrows indicate nuclear RSK2 in control versus cytoplasmic RSK2 with 4-OHT. (Bar, median±quartile, n=2 patients, ≥15organoids/condition) and cyclin D1 (Bar, median±quartile, n=2 patients, ≥8 organoids/condition). The data were normalized to the control. ***p<0.001; Student's t-test.

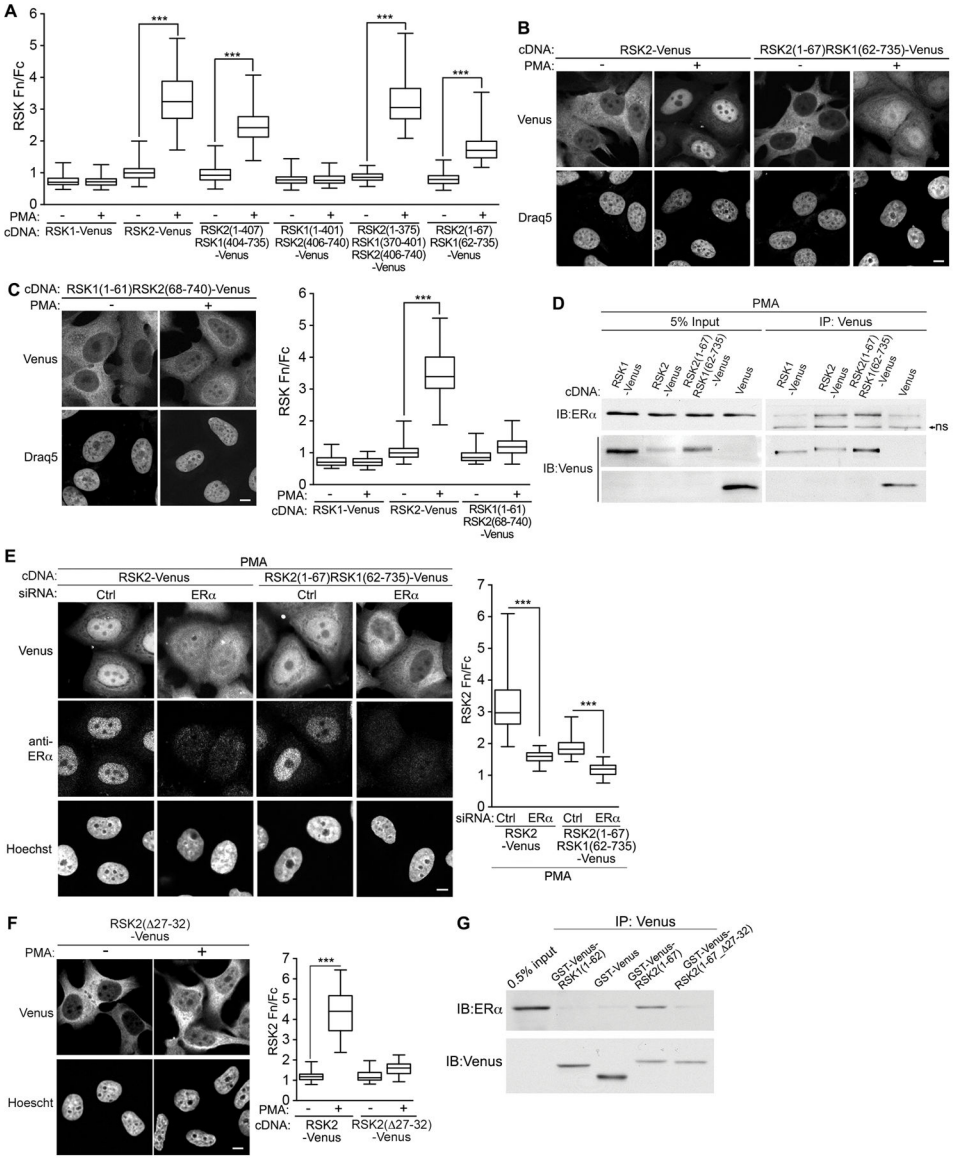

Figure 4. ERα sequesters RSK2 via the extreme RSK2 N-terminus

(A) Nuclear accumulation (Fn/Fc) of RSK constructs. (Bar, median±quartile, n≥3, ≥50 cells/treatment). ***p<0.001 Student's t-test. (B) The extreme N-terminus of RSK2 confers nuclear accumulation. Scale bar=10μm. (C) Replacement of the extreme N-terminus of RSK2 with that of RSK1 prevents nuclear accumulation. (Bar, median±quartile, n≥3, ≥50 cells/treatment). ***p<0.001; Student's t-test. (D) ERα physically associates with the extreme N-terminus of RSK2. MCF-7 cells were transduced, ERK1/2 signaling activated and Venus-tagged and co-associated proteins immunoprecipitated with an anti-Venus antibody. ns=nonspecific. (E) ERα regulates RSK2 nuclear accumulation through residues 1 to 67 of RSK2. MCF-7 cells over-expressing RSK2-Venus or RSK2(1-67)RSK1(62-735)-Venus were transfected with control or ERα-specific siRNA. Scale bar=10 μm. (Bar, median±quartile, n=3, 50 cells/treatment). ***p<0.001; Student's t-test. (F) RSK2 residues from 27 to 32 regulate RSK2 nuclear accumulation. Scale bar=10μm. (Bar, median±quartile,

n=3, ≥50 cells/treatment) ***p<0.001; Student's t-test. (G) ERα associates with purified, recombinant RSK2(1-67), but not with RSK1(1-62) or RSK2(1-67_Δ27-32).

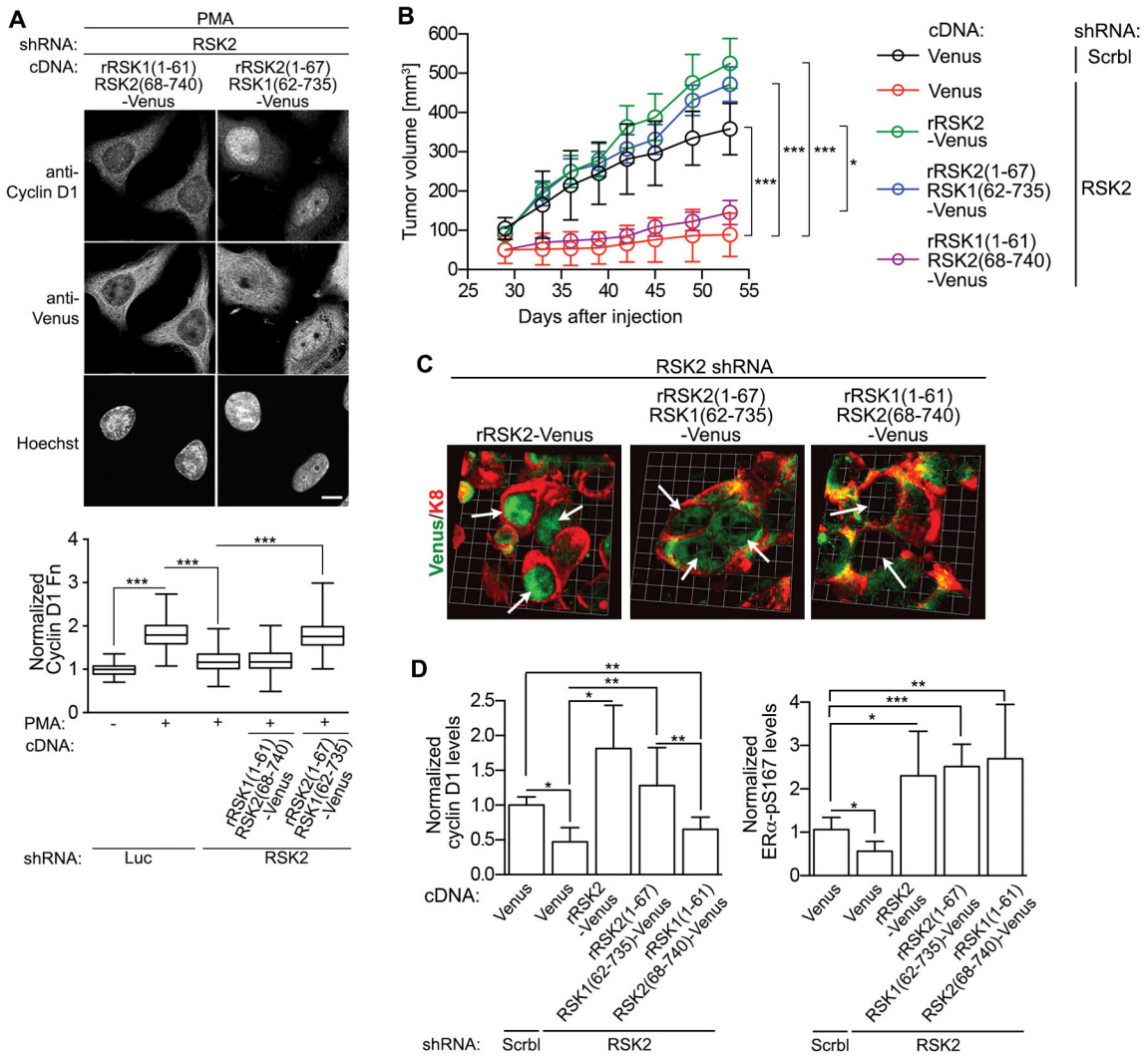

Figure 5. RSK2 nuclear accumulation is required for ER+ tumor growth

(A) Nuclear localization of RSK2 is required for increased cyclin D1 levels. MCF-7 cells were transduced with a control (Luc) or RSK2 shRNA in combination with resistant mutant RSK constructs before stimulation. Scale bar=10μm. (Bar, median±quartile, n=3, ≥78 cells/treatment). ***p<0.001; Student's t-test. (B) ER+ tumor growth is dependent on RSK2 nuclear accumulation. MCF-7 cells transduced with Scrbl or RSK2 shRNA were also transduced with Venus or resistant WT or mutant RSK constructs. Transduced MCF-7 cells were injected into the 4th mammary fat pad of NSG mice implanted with an E_2 pellet. (Symbol, mean±SD, n≥4 mice/group, 2 tumors/mouse) *p<0.05, ***p<0.001; two-way-ANOVA for the last time point; (C) Nuclear accumulation of RSK constructs shown by 3D projections of 6 1μm Z-stack images. Arrows indicate nuclei. (D) RSK2 nuclear accumulation correlates with cyclin D1 but not pSer-167 levels. The samples were normalized to RAN. The data were normalized to the control. (Bar, mean±SD, n=3 tumors (triplicate)). *p<0.05, **p<0.01, ***p<0.001; Student's t-test.

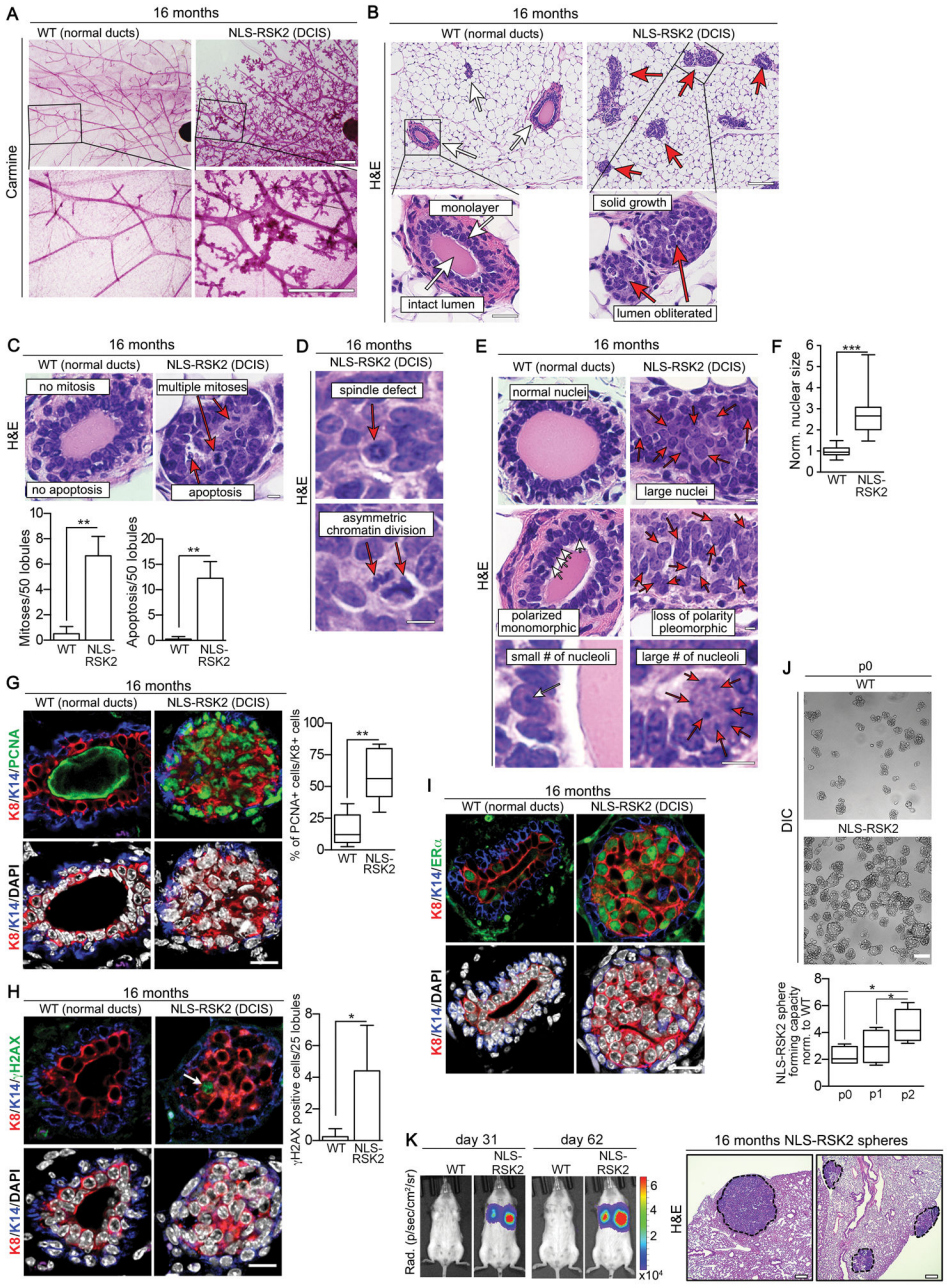

Figure 6. Nuclear RSK2 induces neoplastic transformation of the mammary gland

(A) Carmine stained whole mount images of the 4th mammary gland isolated from sixteen month WT and NLS-RSK2 transgenic mice. Scale Bar=200μm. (B) H&E sections demonstrate ductal filling (red arrows) in the mammary glands of NLS-RSK2 versus normal ducts (white arrows) in WT mice. Scale Bar=100μm. (C) Increased mitosis and apoptosis are observed in the ducts of NLS-RSK2 mice. Scale Bar=10μm (Bar, mean±SD, n ≥4 mice/genotype). **p<0.01; Student's t-test. (D) Examples of mitotic defects in ducts of NLS-RSK2 mice. Scale Bar=10μm. (E) H&E sections of mammary glands from the NLS-RSK2 mice show numerous indications consistent with neoplastic transformation (red

arrows). Scale Bar=10μm. (F) Nuclear size increases in cells within DCIS lesions from NLS-RSK2 mice relative to nuclei from ducts within WT mice. (Bar, median±quartile, n=4 mice/genotype, ≥4 fields/mouse) ***p<0.001; Student's t-test. (G) Increased mitosis within the ducts of the NLS-RSK2 mice, as observed by PCNA staining. Scale Bar=20μm. (Bar, median±quartile, n=4 mice/genotype, ≥5 fields/mouse). **p<0.01; Student's t-test. (H) Increased DNA damage was observed by γH2AX staining within the ducts of the NLS-RSK2 mice. Arrow indicates γH2AX+ cell. Scale Bar=20μm (Bar, mean±SD, n=4 mice/genotype, ≥5 fields/mouse). *p<0.05; Student's t-test. (I) DCIS lesions in NLS-RSK2 mice are ER+. Scale Bar=20μm. (J) Cells from isolated NLS-RSK2 mice demonstrate higher tumor potential than WT. Sphere cultures generated from mammary cells isolated from WT or NLS-RSK2 mice were cultured and passaged (p). Differential interference contrast (DIC) images are shown. Sphere forming capacity was normalized to WT. Scale Bar=50μm (Bar, median±quartile, n=4 mice/genotype, triplicate) *p<0.05, **p<0.01, Student's t-test. (K) Mammary cells expressing NLS-RSK2 generate metastatic lesions when introduced by IC injection. Equal sphere numbers from (J: p0)) were transduced with luciferase and introduced into NCG mice with bioluminescence imaging performed at the indicated time. H&E sections of the lungs from mice injected with NLS-RSK2 spheres show numerous metastatic lesions (outlined). Scale Bar=200μm. (n=3 mice with WT spheres; =4 mice with NLS-RSK2 spheres). p<0.05, Fisher's exact test.